ACS Sustainable Chemistry & Engineering

pubs.acs.org/journal/ascecg

Research Article

Boosting Renewable Methanol Production: A Study on Enriched Hydrogen Recovery Using Hollow Fiber Carbon Membranes in Syngas Stream Upgrades

Adele Brunetti,*,○ Danlin Chen,○ Elisa Avruscio, Linfeng Lei,* Dionysis Karousos, Giuseppe Barbieri, Evangelos P. Favvas,* and Xuezhong He*

Cite This: *ACS Sustainable Chem. Eng.* 2024, 12, 3344−3354

Read Online

ACCESS | Metrics & More | Article Recommendations | Supporting Information

ABSTRACT: Biomass gasification is a viable solution for generating H_2; however, the syngas produced must be upgraded to make H_2-containing streams suitable for other applications, such as renewable methanol production, by adjusting the H_2/CO ratio. In this study, for the first time in the literature, the separation properties of carbon hollow fiber membranes in binary and quaternary H_2-containing mixtures with varying compositions were systematically explored. It was found that the developed carbon membranes exhibit relatively good selectivity for (H_2+CO_2) in mixtures with other gases such as N_2 and CO, which are commonly present in syngas. A CO permeance of 0.8−1 GPU and a H_2/CO selectivity of 30 were achieved for the first time through both single gas and mixed gas permeation testing. Furthermore, in the context of using these membranes for syngas upgrading, such as in an integrated biomass-to-biofuel (methanol) process for hydrogen enrichment or carbon capture and conversion, a technical feasibility analysis based on the separation performance of the carbon membrane system for syngas ratio adjustment and N_2 removal was carried out. The results indicate that the prepared carbon membranes have the potential to adjust the H_2/CO ratio to 1−3 if a N_2 removal ranging from 80 to 90% is acceptable.

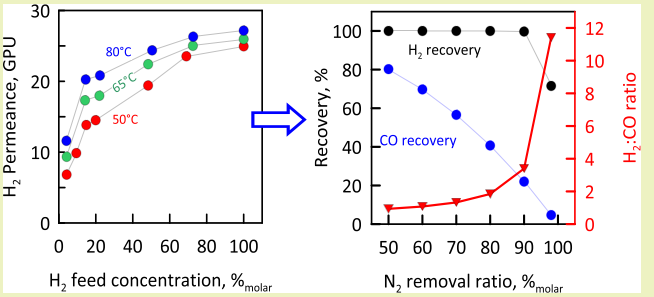

KEYWORDS: *carbon membranes, biomass gasification, H_2/CO ratio adjusting, N_2 removal, gas permeance*

1. INTRODUCTION

Global energy demand is expected to increase exponentially in the coming years with a more and more accretive increase. Following the direction for minimizing the use of fossil fuels, countries have turned their attention to the use of renewable energy sources in addition to fossil fuels to meet their increasing energy needs and obtain clean energy.

Hydrogen is a beacon of hope in the quest to curb CO_2 emissions and mitigate the greenhouse effect.[1,2] As a noncarbon fuel, its combustion yields nothing but water. Currently, global hydrogen demand is primarily driven by ammonia synthesis (51%), oil refining (31%), and methanol synthesis (10%).[3] To meet this demand, approximately 95 million tons of hydrogen are produced annually.[4] The European Commission has set an ambitious target to produce and import 10 million tons of renewable hydrogen by 2030 through water electrolysis, underpinned by the hydrogen accelerator concept.[5] However, hydrogen does not occur naturally in its pure form. It must be extracted from fossil fuels (via steam reforming,[6] partial oxidation, or coal gasification) or renewable sources (via biomass gasification[7] or water splitting using solar/wind energy).[8−12] Hydrogen production technologies are classified into three categories based on their CO_2 emissions: positive, free, and neutral.[13] The most appealing category is neutral CO_2 emissions, which can be achieved using biomass as a feedstock through biological (dark and photo fermentation, biophotolysis) or thermochemical processes (gasification and pyrolysis).[14]

Although gasification is a technique that produces the largest amount of CO_2 and has the highest carbon footprint,[15] it remains one of the most commonly utilized processes for hydrogen production.[16−21] The main reason for this is that most existing industrial plants are large scale, which makes switchover to new technologies slower. In addition, unexpected events, such as the recent global energy crisis, are directing governments to activate solutions for the production of energy based on fossil fuels.[22] Alternatively, transforming raw materials and byproducts, such as coal, wood, plastic waste[23] and solid waste,[24] sawdust, car tires, and sewage sludge into

Received: December 14, 2023
Revised: February 2, 2024
Accepted: February 6, 2024
Published: February 14, 2024

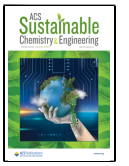

useful outputs of gasification techniques, is considered an applicable solution.[18,25] Through the gasification process, carbon-containing materials are converted into synthesis gas (see Figure S1), which is a gas mixture containing some or all of H_2, CH_4, CO, NH_3, H_2S, N_2, HCl, and HCN and also ash and tar.[26] The typical composition of syngas mixture ranges CO 18−20%, H_2 15−20%, CH_4 1−5%, CO_2 9−12%, and N_2 45−55%, without considering contaminants and other substance, even though it differs depending on fuel type and gasification method. Values for the downdraft method and different gasifier types were reported by Faizan and Song[27] (Table S2).

In order to comply with the directives concerning the reduction of greenhouse gas emissions, development of new, but also improvement of existing, technologies must be given high priority by governments and the scientific community. To this end, research was intensified over the past decade on modes of operating coal-fired power plants with carbon capture and storage. In particular, precombustion options via coal gasification, especially integrated gasification combined cycle processes, are attracting the attention of governments, industry, and research community as a fast-adaptation alternative to conventional power generation.[28] Moreover, the biomass gasification process can also produce syngas, but the challenges and demands of syngas cleaning must be addressed.[29] For example, based on the fact that wood gasification produces a gas mixture with a high concentration of N_2 (Table S2), removing most of N_2, it can lead to a final enriched mixture that could be used for methanol production, given that global methanol capacity is poised to see considerable growth over the next five years, potentially increasing from 171.8 MTPA (million tons per annum) in 2022 to 302 MTPA in 2027, registering a total growth of 75.8%.[30] Industrial production of methanol is currently being carried out by reforming fossil-derived syngas (primary CO and H_2) over metal-based catalysts at 50−100 bar and 200−300 °C. Today, numerous studies also focus on the use of CO_2 instead of CO in methanol synthesis according to the reaction: $CO_2+3H_2 \rightarrow CH_3OH+H_2O$ ($\Delta H^0_{298} = -49$ kJ/mol), even though this is a great challenge given its high activation energy, which demands substantial energy input.[28] If flare gas is used for methanol production, the use of a separation technology able to simultaneously separate CH_4, CO, and N_2 from CO_2 and H_2 could significantly enhance the efficiency of the process, as suggested by Khanipour et al.[31] who proposed the use of selective membranes toward CO_2+H_2 to adjust the H_2/CO ratio, while keeping a high hydrogen recovery after the enrichment. Membrane technology is emerging as a formidable challenge to conventional hydrogen separation techniques, such as pressure swing adsorption and cryogenic distillation. It boasts several advantages, including lower costs, reduced energy consumption, simplicity, and compactness, making it a more economically and environmentally viable option.

It is a well-established fact that there is a wide array of membrane materials available, each with its unique properties, making them suitable for various gas separation processes. This includes a vast selection of polymeric substances, as well as inorganic membranes like zeolitic, ceramic, carbon, and thin-film metallic membranes.[32]

In the commercial sphere, polymeric membranes are dominating. Membrane manufacturers typically use a select group of polymers for hydrogen-selective membrane materials. These include polysulfones, polycarbonates, cellulose acetates, polyphenyloxides, and polyimides. New, tailor-made polymers are under rigorous research and development, but their current cost makes them prohibitive for large-scale use.[33] However, commercial polymeric membranes usually present relatively low selectivity for H_2 purification while inorganic membranes such as the palladium-based or ceramic membranes are highly cost-intensive, which limits their large-scale applications in this field. The emerging carbon membranes showed promising performances for H_2 separation and purification to efficiently separate hydrogen from other larger gas molecules (e.g., CO_2, N_2, CH_4).[34,35] Upon comparing the performance of the carbon membranes proposed in this study to the most commonly used polymer membranes at a commercial level (as shown in Table S3), it becomes clear that the carbon membranes exhibit comparable, if not superior, permeability and selectivity (considering single gas measurements). This is particularly notable in temperature ranges that exceed those typically tolerated by polymer membranes. Furthermore, it is widely recognized that carbon membranes maintain their stability even under high-temperature conditions. Such an environment is a prerequisite for gasification and/or steam methane reforming processes. This underscores the potential advantages of using carbon membranes in these applications. In our previous work,[36] we have demonstrated the capability of hollow fiber carbon membranes to operate stably also in the presence of contaminants and water vapor for more than 180 days of continuous testing. In this work, carbon hollow fiber membranes were developed to selectively separate H_2 and CO_2. These membranes were used to separate H_2 from binary (H_2/CO_2, H_2/CO, and H_2/CH_4) and quaternary (CO_2, N_2, H_2, and CO) mixtures of different feed concentrations and temperatures. The mutual influence of gases in H_2-containing mixtures on membrane permeation and the corresponding variations in separation properties compared with single gas measurements were systematically investigated. This led to a comprehensive understanding of the differences in permeance and selectivity observed in mixed-gas conditions. To the best of our knowledge, this is the first time in literature that the performance of carbon hollow fiber membranes was investigated with H_2 mixtures containing CO and where the wide variation of H_2 behavior has been analyzed based on feed molar fraction composition and the presence of other gases in the mixture.

Experimental results obtained by feeding a quaternary mixture with the typical composition of syngas as produced in a biomass gasifier reactor were used as input for technology feasibility analysis simulations. UNISIM simulation integrated with a customized membrane unit was applied to investigate the potential for adjusting the H_2/CO ratio and removing N_2 using the prepared carbon membranes.

2. MATERIALS AND METHODS

2.1. Membrane Preparation. Microcrystalline cellulose (MCC, Avicel PH-101) was used as a polymer precursor for carbon hollow fiber membranes. Specifically, the MCC was dissolved into a cosolvent of 1-ethyl-3-methylimidazolium acetate (EmimAc, >95%, purchased from IoLiTec GmbH) and dimethyl sulfoxide (DMSO, purchased from Sigma-Aldrich) at 60 °C. The weight ratios of MCC, EmimAc, and DMSO were controlled at 12, 66, and 22%$_{wt}$, respectively. The cellulose hollow fiber membrane precursors were then fabricated by a dry-wet spinning during which a bore solution consisted of 80%$_{wt}$ cosolvent and 20%$_{wt}$ ID water. Before being dried in a lab atmosphere with a temperature of ca. 25 °C relative humidity of ca. 30%, the as-spun fresh cellulose hollow fibers were soaked in

https://doi.org/10.1021/acssuschemeng.3c08236
ACS Sustainable Chem. Eng. 2024, 12, 3344−3354

water for 72 h to remove residual cosolvent. Afterward, the precursors were carbonized with an argon purge gas using the carbonization procedure described elsewhere.[36,37] The asymmetric carbon membranes with an average thickness for the selective layer of 3 μm were successfully prepared and reported in the previous work[37,38] (Figure S3). A hollow fiber membrane module containing five carbon hollow fiber membranes with an effective membrane area of 9.5 cm^2 was then constructed in a 3/8 in. stainless steel tube sealed by epoxy adhesive, which was used for gas permeation testing.

2.2. Mass Transport Property Evaluation. The separation properties of the carbon-based membranes were explored in the temperature range 50−80 °C for H_2, N_2, CO_2, CH_4, and CO as single gas and in mixtures (Table 1) at a feed pressure of 10 bar. The experimental setup used for the experiments is shown in Figure 1.

Table 1. Operating Conditions Used in the Experimental Measurements

temperature (°C)	50−65−80
feed pressure, bar	up to 10 bar
permeate pressure, bar	1−1.2
sweep gas flow rate, mL(STP) min^{-1}	5
feed flow rate, mL(STP) min^{-1}	100−500
single gas (purity 5.0)	H_2, CO_2, CH_4, CO
sweep gas (purity 5.0)	N_2
gas mixture composition (molar %)	H_2:CO_2 = 65:35
	H_2:CO_2 = 50:50
	H_2:CO_2 = 85:15
	H_2:CO = 70:30
	H_2:CO = 50:50
	H_2:CO = 20:80
	H_2:CH_4 = 5:95
	H_2:CH_4 = 10:90
	H_2:CH_4 = 20:80
	H_2:CH_4 = 50:50
	CO_2:H_2:N_2:CO = 15.1:14.2: 55.4:16.3
	CO_2:H_2:N_2:CO = 15.7: 3.5:58.9:21.8
	CO_2:H_2:N_2: CO = 18.9: 4.2:20.2:56.6

The hollow fiber membrane module was placed in a furnace for precise temperature control. Mass flow controllers (Brooks Instruments 5850S) were used to regulate the flow rate of gases fed to the module. Gas mixtures were either already available in certified bottles or modulated using mass flow controllers. A back pressure controller (Swagelok KBP series) regulated feed pressure, and pressure drops were monitored using gauges on the feed and retentate lines. Temperature was finely monitored by using sensors on the feed, retentate, and permeate lines (Digitron HLX31PFTE). During single and binary mixed gas experiments, a constant N_2 sweep gas flow rate of 5 mL(STP) min^{-1} was applied. This was done primarily for two reasons: first, due to the limited membrane area, the resultant permeate flow rate is inherently low; second, the introduction of a sweep gas serves a dual purpose. It not only enhances the driving force, thereby enhancing the flux, but also ensures a consistent and quantifiable flow rate for the microgas chromatograph. Permeate pressure was atmospheric for single gas measurements or slightly higher for mixtures owing to pressure drop from the microgas chromatograph.

Separation measurements were carried out under steady-state conditions, and the membrane module was exposed to a nitrogen stream at a pressure of 10 bar during stand-by periods or changes in operating conditions. Before changing gas supply, the module was "washed" by feeding the new gas/mixture for 30 min on both sides of the membrane. The composition of permeate, retentate, and feed was analyzed using a micro gas chromatograph (Agilent 990) equipped with different columns (Molsieve 5 Å, PoraPLOT Q, CP-Sil 19 CB) and three TCDs.

Almost all the results reported in this paper showed a standard deviation below 4%. The figures show error bars only when the error exceeds this value.

The separation properties of the membrane were evaluated in terms of permeance, permeability, and selectivity. Permeance (GPU, 1GPU= 2.736×10^{-3} m^3(STP)/(m^2 h bar) is the ratio of permeating flux (m^3(STP)/(m^2 h) and the partial pressure differences (bar) between the two membrane sides (eq 1):

$$\text{permeance}_i = \frac{\text{permeating flux}_i}{\Delta P_i} \tag{1}$$

All the permeation measures with mixed gases were carried out to guarantee a stage cut lower than 1%. This condition assured the absence of relevant partial pressure profiles in the two membrane sides, and we calculated the driving force by using eq 2 and selectivity ($\alpha_{i/j}$) as the ratio between the gas permeability of the two gases, also in mixed gas conditions (eq 3).

$$\overline{\Delta P_i} = \left[\left(\frac{P_i^{\text{feed}} + P_i^{\text{retentate}}}{2}\right) - \left(\frac{P_i^{\text{permeate}} + P_i^{\text{sweep}}}{2}\right)\right], \text{ bar} \tag{2}$$

$$\alpha_{i/j} = \frac{\text{permeance}_i}{\text{permeance}_j} \tag{3}$$

2.3. Process Design and Simulation Basis. Concerning the small-scale scenario of syngas production from the gasification process, a single-stage carbon membrane system with a syngas processing capacity of ≤1000 N m^3 h^{-1} was designed, as described in Figure 2. Ahead of introducing the syngas stream delivered from the gasification process into the membrane unit, it is initially pressurized to 8 bar and adjusted to a desired operating temperature (Table 2). The membrane area can be modulated to produce the syngas with an optimal H_2:CO ratio at a given N_2 removal ratio, while the pressure of the retentate stream is maintained constant with the feed pressure. Compressors are necessary for both the feed and retentate sides of the membrane unit, while a vacuum suction pump is required on the permeate side. It should be noted that the present study does not incorporate the heat integration network between the condenser and heat exchanger—this aspect might be explored in future work.

On the basis of the separation performance of the fabricated carbon membrane and the aforementioned process description, the simulation basis described in Table 2 was employed to assess the technical feasibility of the carbon membrane system in terms of adjusting the syngas ratio and removing N_2 from the gasification process. A typical syngas composition consisting of CO_2, H_2, CO, and N_2 in a molar ratio of 15:15:20:50 was adopted while the presence of CH_4 in negligible quantities was ignored to streamline the process simulation. The process described in Figure 2 was simulated using the UNISIM simulation software, which is integrated with a tailored membrane model configured featuring a counter-current flow pattern.[39] A 1D, first-order model considering a plug-flow on both membrane sides was implemented, meaning no concentration gradients in the radial direction. In addition, no pressure drops on feed and permeate sides were accounted. Given that removing a significant portion of N_2 in the syngas stream is proposed in this study, a N_2 removal ratio of 90% was assumed in the simulation process and the obtained product exhibits potential as a valuable syngas source for downstream methanol and diesel fuel production.[40] Moreover, the pressure drops associated with coolers and heat exchangers were not taken into consideration and an adiabatic efficiency of 75% was applied to estimate the energy demand of compressors and vacuum pumps. A comprehensive analysis was carried out on the process parameters including operating temperature and vacuum pressure as well as a sensitivity analysis of the N_2 removal ratio, based on the experimental data acquired from the

https://doi.org/10.1021/acssuschemeng.3c08236
ACS Sustainable Chem. Eng. 2024, 12, 3344−3354

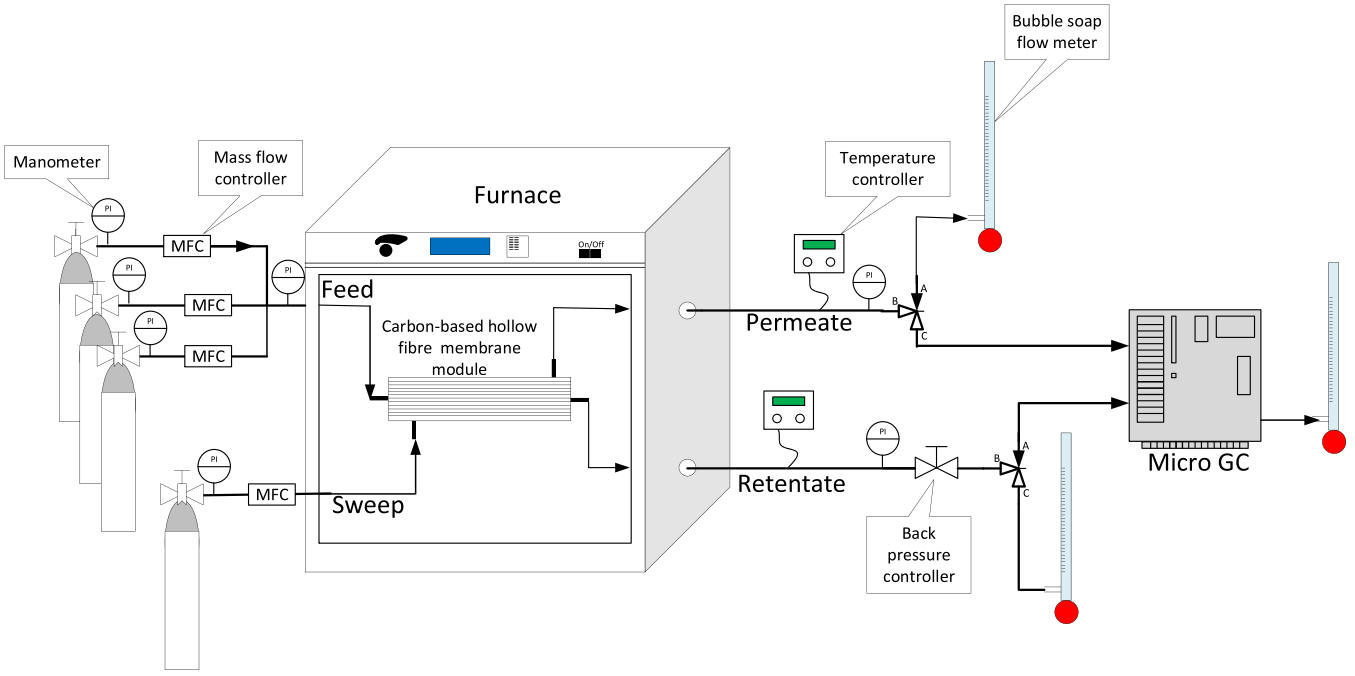

Figure 1. Experimental setup for the gas permeation measurements.

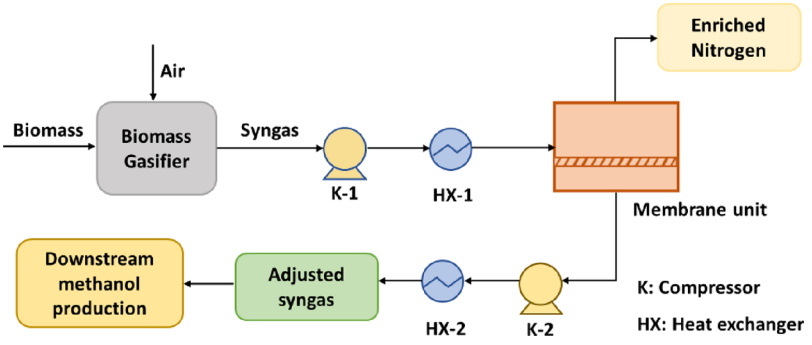

Figure 2. The schematic illustration of the single-stage membrane system for syngas ratio adjustment and N_2 removal.

Table 2. Simulation Basis for the Single-Stage Membrane System

parameters	value
feed gas flow, m^3(STP) h^{-1}	1000
feed pressure, bar	8
permeate pressure, kPa	10−50
operating temperature, °C	50−80
N_2 removal ratio, %	90
membrane performance	based on Figure 9b

quaternary gas permeation test. It is noteworthy that the gas permeance was assumed to remain constant along the membrane module. Additionally, for the sake of simplifying the simulation, any impacts stemming from variations in feed pressure resulting from the application of sweeping and vacuuming on the permeate side were disregarded.

3. RESULTS AND DISCUSSION

3.1. Single Gas Permeation Performance. The gas permeation measurements were carried out to investigate the capability of the membranes to separate H_2-containing mixtures with different species and compositions and to understand how their permeation is influenced by the presence of other gases. To this end, single gas permeances of H_2, CO_2, CO, and CH_4 were initially measured at different temperatures to serve as references for quantifying their behavior in mixed gas conditions. Since the sweep gas used in the single gas measurements was nitrogen itself, it was not possible to determine its permeance due to the low permeate flow, which did not allow for a concrete reproducibility in measuring the flow difference compared to the sweep flow. The permeance of all single gases increased with temperature, with H_2 being the most permeable gas, followed by CO_2, CO, and CH_4 (Table 3). This agrees with what has already been observed in the literature,[41−43] where permeability is inversely proportional to the critical volume of the molecules, confirming that diffusion

Table 3. Permeances of Single Gases as a Function of Temperature

	permeance, GPU			
temperature, °C	H_2	CO_2	CO	CH_4
50	22.2	4.3	0.7	0.17
65	25.8	4.7	0.8	0.19
80	27.2	6.0	0.8	0.22

https://doi.org/10.1021/acssuschemeng.3c08236
ACS Sustainable Chem. Eng. 2024, 12, 3344−3354

is the dominant transport mechanism (Figure 3a). We evaluated the separation properties of the membranes in the presence of three different binary H_2 mixtures (H_2 mixed with CO_2, CO, and CH_4) at various compositions and three quaternary mixtures also containing H_2, but with a composition closer to real syngas streams, as detailed in Table 1.

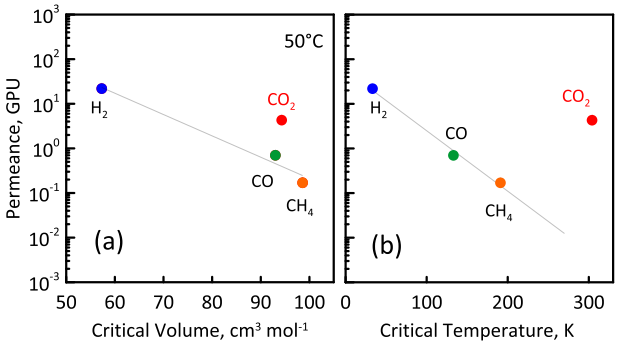

Figure 3. Permeance of single gases as a function of their related (a) critical volume and (b) critical temperature at 50 °C.

3.2. Mixed Gas Separation Performance. *3.2.1. Feed Gas Content Influences.* For all binary mixtures, H_2 was the most permeable gas. However, when mixed, its permeance was always lower than that measured as a single gas (Figure 4). When examining the H_2:CO_2 mixture, which includes the most permeable gases among those considered in this work, we found that the H_2 permeance decreased as the fraction of CO_2 in the feed increased. On the other hand, CO_2 permeance was always higher than that measured in single gas and tended to increase as the concentration of H_2 in the feed increased, reaching its highest value when the mixture contained about 80% H_2. A similar behavior has been observed experimentally and theoretically for zeolite membranes for both H_2 and CO_2 trends.[44,45] As already observed in literature,[36] even though permeation through carbon membranes is primarily controlled by diffusion into pores of size comparable with the molecule size, the reduction of H_2 permeance with increasing CO_2 feed molar fraction can be attributed to the hindering effect of CO_2 molecules preferentially adsorbed on the sorption sites of the membrane pores.[36] This creates a "reduction" in the volume

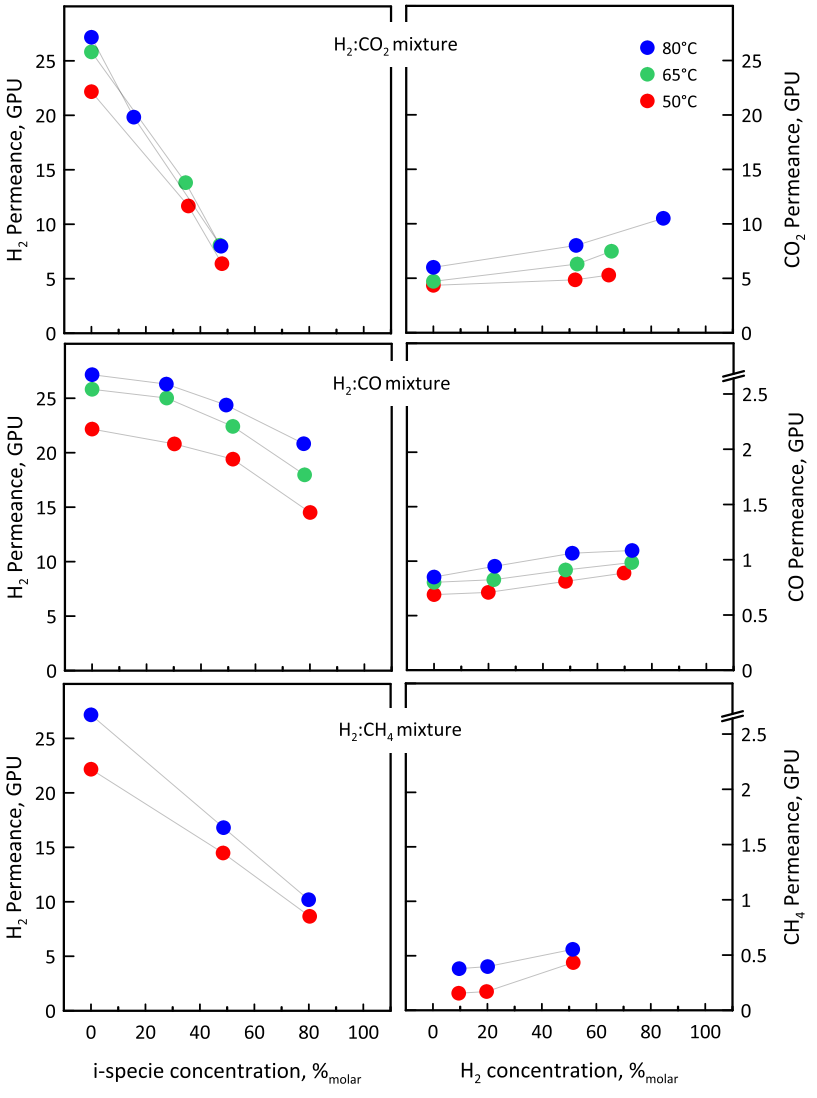

Figure 4. H_2 and i-specie permeances as a function of i-specie concentration in the feed for different H_2-containing binary mixtures.

https://doi.org/10.1021/acssuschemeng.3c08236
ACS Sustainable Chem. Eng. 2024, 12, 3344−3354

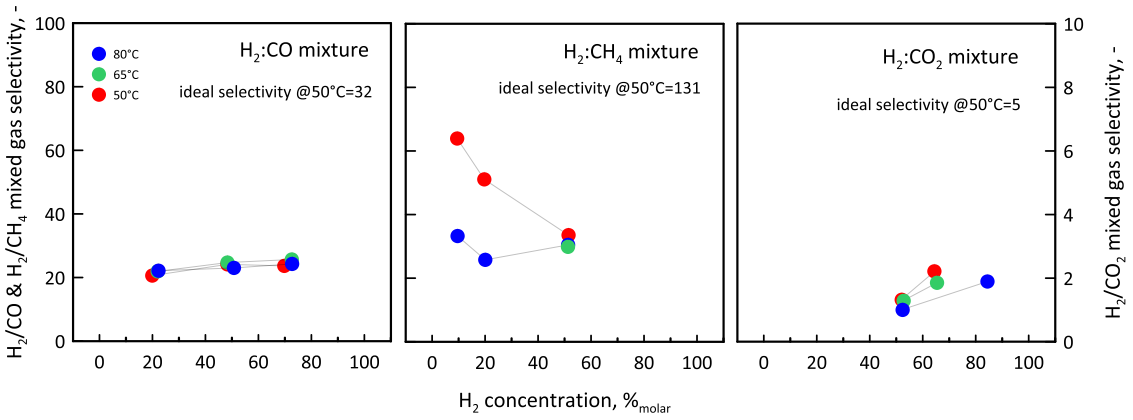

Figure 5. Mixed gas selectivity as a function of the H_2 concentration in the feed for different H_2-containing binary mixtures.

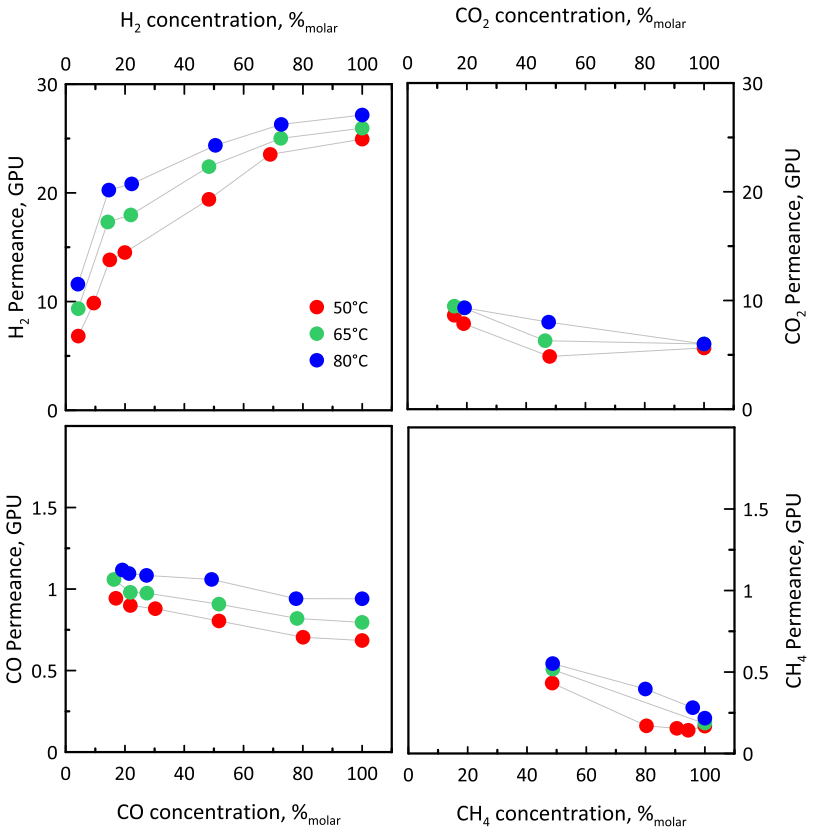

Figure 6. Permeance of H_2, CO_2, and CO and CH_4 as a function of their concentration in the feed for different H_2-containing (binary and quaternary) mixtures (Table 1) at different temperatures.

available for the diffusion of molecules, resulting in a decrease in the H_2 permeance. With the increasing of the H_2 feed molar fraction, less CO_2 is present in the feed and thus it easily adsorbs inside the membrane matrix, with a consequent increase in CO_2 diffusivity owing to the reverse of coverage,[46,47] which is dominant over the lower sorption, resulting in an increase in CO_2 permeance. A similar behavior was observed for the other binary mixtures of H_2 with CO or CH_4. In both cases, H_2 permeance decreased with respect to single gas conditions as the molar fraction of the other component in the mixture increased, while the permeance of CO and CH_4 increased as the H_2 concentration increased. Overall, compared to the H_2:CO_2 mixture, the reduction effect on H_2 permeance was less significant.

In particular, when considering a feed stream at 50 °C containing 50% H_2 and 50% of the other gas, the reduction of H_2 permeance in the mixture with CO_2 was about 70%, compared to 34 and 11% with CH_4 and CO, respectively. Looking at the other gases in an equimolecular mixture with H_2, CO permeance was enhanced by about 18% and CO_2 of 12%, while CH_4 permeance was 2.6 times the one in single gas conditions.

The differences in the mutual interactions among different gases can be attributed to their permeance and ability to be sorbed in membrane pores. As previously mentioned, CO_2 is the most permeable gas after H_2 and also has a good ability to be sorbed in the carbon membrane, resulting in a significant hindering effect on H_2 and being positively affected by the

https://doi.org/10.1021/acssuschemeng.3c08236
ACS Sustainable Chem. Eng. 2024, 12, 3344−3354

binary diffusivity, which deviates from the CO_2 single gas diffusivity, making CO_2 diffusion faster in H_2 mixtures. In the case of CO and CH_4, their permeances are very low compared to that of CO_2, so less gas can be present in the carbon membrane during permeation. This implies, as confirmed by results in Figure 4, a less significant effect on H_2 permeance, which, on the contrary, exerts a much more significant promoting effect on the permeation of CO and CH_4 permeation. A further distinction can be made between the effects of CO and CH_4. Even though their permeances are comparable, the effect of CH_4 on H_2 permeance is more evident than that of CO and this can also be attributed to the different affinity of the gas with the carbon matrix. CH_4 has a solubility in carbon-based membranes[36] that is about 66% that of CO_2, so it can also exert a hindering effect similar to that of CO_2, but less significant.

This is confirmed by the fact that in the presence of CO_2, H_2 permeance is reduced by about 70% while with CH_4, its reduction is about 34%. We were unable to measure the solubility of CO owing to limitations of our apparatus. However, by looking at the critical temperature (Figure 3b), which can be considered an indirect indication of the affinity of the molecule to be sorbed in the membrane matrix, one could expect that its solubility contribution is less significant than that of CH_4, justifying its lesser impact on H_2 permeance.

The different behaviors observed regarding the permeation of various gases in mixed gas conditions were reflected in significant variations of selectivity values for the various mixtures investigated (Figure 5). All binary mixtures displayed lower selectivities than their single gas counterparts. This was due to the increase of both permeances with the H_2 molar fraction and was more pronounced at lower temperatures.

However, while the H_2:CO_2 mixture selectivity increased with the H_2 concentration, the other mixtures behaved differently. When mixed with CO, selectivity remained stable as a compromise of the permeance variation of the two gases that was almost similar as the hydrogen molar fraction increased. In contrast, the H_2:CH_4 mixture showed an overall decrease in selectivity, particularly at 50 °C. This was owing to the promotional effect of H_2 on CH_4 permeation and the hindering effect of CH_4 on the H_2 one. As the temperature increased, H_2 diffusion was enhanced while CH_4 sorption decreased, resulting in less variation in selectivity.

We performed additional tests on three quaternary mixtures with varying compositions (CO_2:H_2:N_2:CO = 15.1:14.2:55.4:16.3; CO_2:H_2:N_2:CO = 15.7:3.5:58.9:21.8; CO_2:H_2:N_2:CO = 18.9:4.2:20.2:56.6). In this case, we used CH_4 as the sweep gas to better distinguish the permeating flux of N_2. Interestingly, when we plotted the permeances of H_2, CO, and CO_2 against their molar fractions in the feed together with those measured with all binary mixtures (Figure 6), we found that the permeance trends observed in binary mixtures were also present in quaternary mixtures with different compositions.

Specifically, as the concentration of H_2 in the feed increased, so did its permeance owing to its dominant diffusion compared to other gases. On the other hand, just like with binary mixtures, the permeances of CO_2, CO, and CH_4 decreased as their molar fractions increased, approaching the single gas value owing to the reduced promotional effect of H_2 in the mixture.

3.2.2. Temperature Influences. As expected, the permeance of H_2 increased with temperature, both in a single gas and in mixtures. Its value was always dependent on the influence exerted by the other gases present in the mixture (Figure 7a).

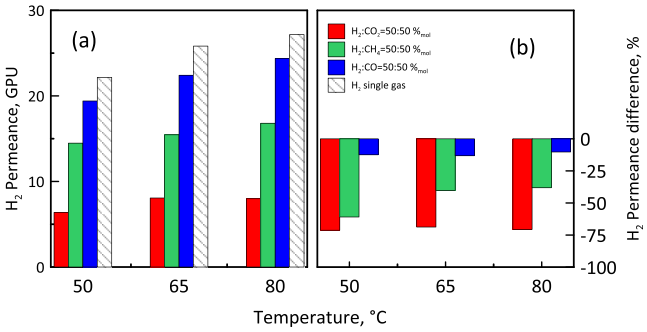

Figure 7. (a) Permeance of H_2 as a single gas and (b) H_2 permeance difference with respect to a single gas in equimolecular mixtures with different gases as a function of temperature.

Therefore, when mixed with CO_2, the variation in permeance with respect to single gas values was always much more significant than that when mixed with CH_4 and CO (Figure 7b). However, the reduction in permeance was less significant as the temperature increased, owing to the promotional effect on H_2 diffusion and the reduced solubility of other gases (CO_2, CH_4, and CO) in the membrane induced by the temperature increase. The permeances of CO_2, CH_4, and CO (Figure 8) also increased and those measured in mixture with H_2 in equimolecular concentration were always higher than single gas. In this case, as already mentioned above, the presence of H_2 caused an enhancement of permeance with respect to a single gas value that was much more significant at higher temperatures, as a consequence of increased H_2 diffusion and thus a more relevant promotional effect on binary diffusivity of the mixture.

3.2.3. Enriched Hydrogen Stream in the Upgrading of Syngas. Based on the results obtained, the hollow fiber carbon-based membranes presented in this study exhibit preferential selectivity toward H_2 and CO_2, with selectivity values that vary depending on the operating conditions and feed composition. As such, they are promising candidates for use in syngas upgrading, such as in an integrated biomass-to-biofuel (methanol) process for hydrogen enrichment or carbon capture and conversion. When examining the permeate compositions obtained from upgrading a typical syngas mixture (Table 1) produced in a biomass gasification reactor,[48] it is evident that the carbon-based membranes significantly increase the concentrations of H_2 and CO_2, which in the feed were 15.1 and 14.2%, while substantially reducing the fraction of N_2 and CO, which ranges between 1 and 3.3% (Figure 9a). In particular, the CO_2 concentration ranged from 63.8 to 64.6% and the H_2 concentration ranged from 34.1 to 29.1% at 50 and 80 °C, respectively. The increase in CO and N_2 concentrations in the permeate with temperature is owing to the increased permeance of these two gases and the concurrent decrease in CO_2 permeance, which is ascribable to the diminished effect of solubility at higher temperatures (Figure 9b).

3.3. Simulation Analysis. The influence of operating temperature on key parameters (e.g., membrane area and power demand) of a single-stage membrane unit used for treating 1000 N m^3 h^{-1} of syngas was examined under the specific conditions of a 90% N_2 removal ratio and a vacuum pressure of 20 kPa at the membrane permeate side. As

https://doi.org/10.1021/acssuschemeng.3c08236
ACS Sustainable Chem. Eng. 2024, 12, 3344−3354

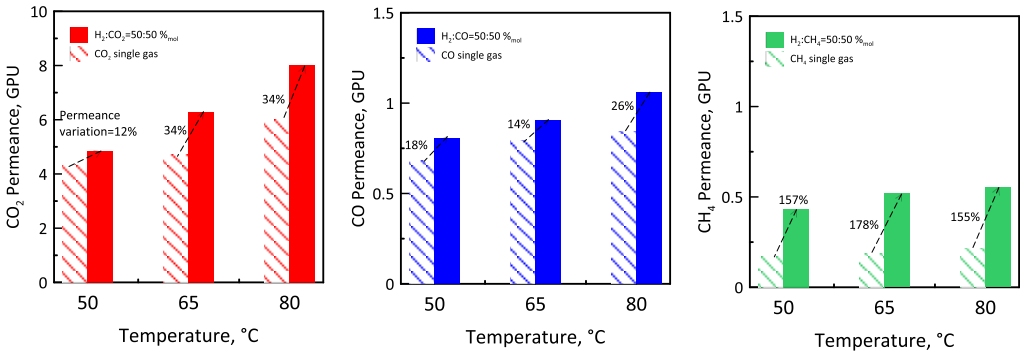

Figure 8. CO_2, CO, and CH_4 permeance as single gas and in equimolecular mixtures with H_2 as a function of temperature.

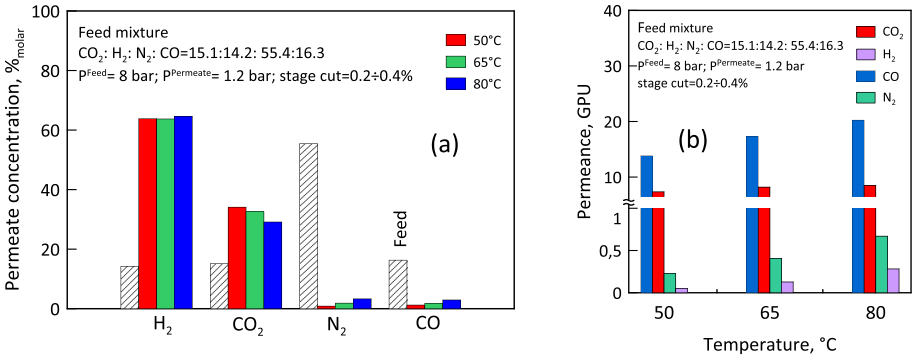

Figure 9. (a) Permeate composition for a typical syngas mixture at three different temperatures and (b) membrane permeance for a quaternary gas permeation test at different temperatures.

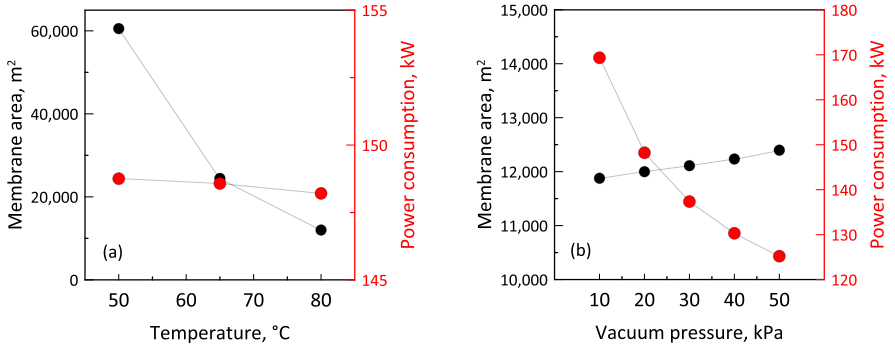

Figure 10. The effects of (a) operating temperature and (b) vacuum pressure on the membrane area and power consumption at 80 °C.

depicted in Figure 10a, a considerably larger membrane area of 60,539 m^2 at 50 °C is necessary in order to offset the reduction in N_2 permeance at lower temperatures, in contrast to the comparatively smaller membrane area of 11,999 m^2 required at 80 °C. Although the permeances for all gas compositions at elevated temperatures are improved, there is a slight decrease in the CO/N_2 selectivity, which brings about a higher CO loss at a given N_2 removal ratio. Consequently, the gas flow rate on the permeate site declines, leading to a marginal reduction in power consumption from 148.7 to 148.2 kW. Figure 10 exhibits the impact of vacuum pressure on the required membrane area and power consumption, considering the best membrane performance at 80 °C and a specified N_2 removal ratio of 90%. Specifically, the required membrane area experiences a slight increase, ranging from 11,877 to 12,397 m^2, as the vacuum pressure varies from 10 to 50 kPa. Conversely, the power demand demonstrates a general downward trend, decreasing from 169.3 to 125.2 kW in response to a progressive rise in vacuum pressure. A greater transmembrane pressure provides a boosted driving force for gas permeation, contributing to a raised permeate flux, along with a lower membrane area. Besides, the increasing gas flux leads to a notable augmentation in the power consumption of both the vacuum pump and the compressors. Overall, the comprehensive examination of operating temperature and vacuum pressure provides valuable insights into the interplay of key parameters within the membrane-based system, contributing to optimizing the system design, enhancing energy efficiency, and ultimately advancing the feasibility of this technology for further practical application.

The investigation places significant emphasis on the N_2 removal ratio owing to the potential impact of N_2 impurities on conversion efficiency for downstream methanol production.[40] N_2, a prevalent impurity, can reduce the partial pressure and hinder the conversion process, necessitating a sensitivity analysis. Additionally, the substantial volume occupied by N_2

https://doi.org/10.1021/acssuschemeng.3c08236
ACS Sustainable Chem. Eng. 2024, 12, 3344−3354

within the reactor incurs higher capital investment costs. As such, a comprehensive sensitivity analysis of the N_2 removal ratio (50−98%) was performed to further evaluate the technical feasibility of the membrane system to produce an enriched gas mixture with a desired H_2/CO ratio under the conditions of the optimal membrane performance at 80 °C and a vacuum pressure of 20 kPa.

As depicted in Figure 11, it can be observed that both the required membrane area and power demand reveal a strong

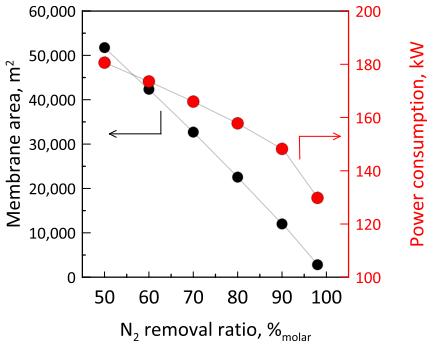

Figure 11. Sensitivity analysis of the N_2 removal ratio on membrane area and power consumption.

dependence on the N_2 removal ratio. An elevated N_2 removal ratio contributes to a lower flow rate of the permeate stream, thereby causing a considerable decrease in both the required membrane area (from 51,740 to 2801 m^2) and power consumption (from 180.6 to 129.8 kW). Furthermore, it is worth noting that the recovery of both H_2 and CO experiences a substantial drop when the desired N_2 removal ratio exceeds 90%, triggering a drastic increase of the H_2:CO ratio in the produced syngas, as highlighted in Figure 12a. Besides, the

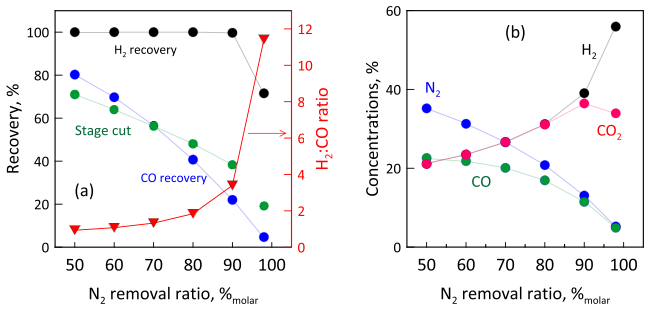

Figure 12. Sensitivity analysis of N_2 removal ratio on (a) gases recovery, stage-cut and H_2/CO ratio, and (b) syngas product enrichment.

stage cut of the membrane system undergoes a notable reduction with the increase of the N_2 removal ratio, attributable to a considerable decrease in the required membrane area. Moreover, the gas concentration in the product stream is depicted in relation to the increased N_2 removal ratio, as shown in Figure 12b, where an enrichment toward CO_2+H_2 is achieved while maintaining moderate CO_2+H_2 recovery. To mitigate excessive CO loss and capitalize on the benefits of CO presence in syngas for downstream applications, it is recommended to target a N_2 removal ratio range of 80 to 90%. This range holds the potential for fine-adjusting the syngas ratio to achieve an optimal H_2:CO ratio of approximately 2−3. Concerning the inadequate membrane performance in separating CO and N_2, future efforts to advance CO-selective membrane materials, enhancing the CO/N_2 selectivity, will be pivotal in reducing the required membrane area while maintaining a high N_2 removal ratio. Additionally, exploring optimized multistage membrane systems could further diminish both membrane area requirements and power demands. Last but not least, a further economic evaluation, considering a notable improvement in membrane performance, can also be undertaken to assess the capital and operational expenditures associated with implementing the membrane system for syngas ratio adjustment and N_2 removal ratio in a practical scenario.

4. CONCLUSIONS

In this study, we explored the use of carbon hollow fiber membranes prepared from cellulose precursors for the separation of H_2 from binary and quaternary mixtures. Our systematic analysis of the separation properties of these carbon hollow fiber membranes in H_2-containing mixtures confirmed that both the permeance and selectivity of mixed gases depend on the type, composition, and temperature of the mixture being treated. Overall, the presence of H_2 in the mixture enhances the permeance of other gases owing to a promotional effect on diffusivity, which deviates from single gas values and accelerates the diffusion of other gases in H_2 mixtures. This effect is more pronounced at higher molar fractions of H_2 in the mixture and at higher temperatures. The presence of CO_2, CH_4, or CO tends to reduce H_2 permeance owing to a hindering effect caused by gas sorption in the carbon membrane, which is more significant at lower H_2 concentrations in the feed and at lower temperatures. Our experiments with quaternary mixtures confirmed that the developed carbon membranes exhibit good selectivity for (H_2+CO_2) in mixtures with other gases such as N_2, CH_4, and CO, which are commonly present in syngas produced from typical biomass gasification processes.

Process simulations were, thus, executed to analyze the technological feasibility of single-stage carbon membrane systems for N_2 removal and syngas ratio adjustment from a typical syngas stream produced by biomass gasification. An appreciable increase in the required membrane area and a reduction in power consumption were observed at a desired higher N_2 removal ratio; however, the enriched syngas product recovery experiences a drastic decline when the N_2 removal ratio exceeds 90%, indicating that the escalated costs associated with pursuing an excessively high N_2 removal ratio may not adequately offset the benefits of space-saving for the downstream reactor and the overall syngas conversion efficiency. Consequently, cost minimization should be carried out in future work to identify the optimal N_2 removal ratio. Considering the substantial membrane area requirement indicated in this simulation study, it is anticipated that a notable enhancement in H_2 and CO permeance could lead to a notable reduction in the required membrane area. Additionally, it is essential to emphasize the significant CO loss for the designed membrane system, which also underscores the urgency for future endeavors dedicated to advancing the development of membranes with elevated H_2 and CO permeances as well as excellent CO/N_2 selectivity to further improve the competitiveness of carbon membranes for this application.

https://doi.org/10.1021/acssuschemeng.3c08236
ACS Sustainable Chem. Eng. 2024, 12, 3344−3354

■ ASSOCIATED CONTENT

Supporting Information

The Supporting Information is available free of charge at https://pubs.acs.org/doi/10.1021/acssuschemeng.3c08236.

Hydrogen color codes, sources, and their carbon footprints; biomass gasifier regions; gas composition (v/v %) from various gasifier types; comparison among carbon membranes belonging to this work and the most used polymer membranes at the commercial level for H_2 separation; and SEM and HR-TEM images of carbon hollow fiber membranes (PDF)

■ AUTHOR INFORMATION

Corresponding Authors

Adele Brunetti − *National Research Council - Institute on Membrane Technology (CNR-ITM), Rende, Cosenza 87036, Italy;* orcid.org/0000-0003-4545-6637; Email: adele.brunetti@cnr.it

Linfeng Lei − *State Key Laboratory of Chemical Engineering, School of Chemical Engineering, East China University of Science and Technology, Shanghai 200237, China;* Email: linfeng.lei@ecust.edu.cn

Evangelos P. Favvas − *National Center for Scientific Research "Demokritos", Institute of Nanoscience and Nanotechnology, Athens 153 41, Greece;* Email: e.favvas@inn.demokritos.gr

Xuezhong He − *Department of Chemical Engineering, Guangdong Technion-Israel Institute of Technology (GTIIT), Shantou 515063, China; The Wolfson Department of Chemical Engineering, Technion - Israel Institute of Technology, Haifa 32000, Israel; Guangdong Provincial Key Laboratory of Materials and Technologies for Energy Conversion, Guangdong Technion - Israel Institute of Technology, Shantou, Guangdong 515063, China;* orcid.org/0000-0002-3232-4945; Email: xuezhong.he@gtiit.edu.cn

Authors

Danlin Chen − *Department of Chemical Engineering, Guangdong Technion-Israel Institute of Technology (GTIIT), Shantou 515063, China*

Elisa Avruscio − *National Research Council - Institute on Membrane Technology (CNR-ITM), Rende, Cosenza 87036, Italy; Department of Environment Engineering, The University of Calabria, Rende, Cosenza 87036, Italy*

Dionysis Karousos − *National Center for Scientific Research "Demokritos", Institute of Nanoscience and Nanotechnology, Athens 153 41, Greece*

Giuseppe Barbieri − *National Research Council - Institute on Membrane Technology (CNR-ITM), Rende, Cosenza 87036, Italy;* orcid.org/0000-0001-5583-8634

Complete contact information is available at: https://pubs.acs.org/10.1021/acssuschemeng.3c08236

Author Contributions

○A.B. and D.C. contributed equally.

Notes

The authors declare no competing financial interest.

A.B.: conceptualization, investigation, formal analysis, writing—original draft preparation, writing— reviewing and editing, supervision, funding acquisition. D.C.: investigation, formal analysis, writing—original draft preparation. E.A.: data acquisition, data analysis. L.L.: writing—original draft preparation. G.B.: reviewing and editing, funding acquisition. D.K. and E.P.F.: writing—reviewing and editing. X.H.: conceptualization, supervision, funding acquisition, writing—reviewing and editing.

■ ACKNOWLEDGMENTS

A.B. and G.B. acknowledge the project "Hydrogen demo Valley: Multifunctional infrastructures for the experimentation and demonstration of hydrogen technologies. 'Mission Innovation' − Scientific Agreement" (21A03302) (GU Serie Generale n.133 del 05-06-2021) between MISE and ENEA for cofunding this work. The authors L.L., E.P.F., and X.H. acknowledge the CO_2Hing project from the Research Council of Norway. X.H. acknowledges the High-level Foreign Expert Bring-in Plan (G2022030037L) from the Ministry of Science and Technology of China and Shenzhen Science and Technology Innovation Commission (G2022019A) for supporting this work.

■ REFERENCES

(1) Schitea, D.; Deveci, M.; Iordache, M.; Bilgili, K.; Akyurt, İ.Z.; Iordache, I. Hydrogen mobility roll-up site selection using intuitionistic fuzzy sets based WASPAS, COPRAS and EDAS. *Int. J. Hydr. Energy* **2019**, *44*, 8585−8600.

(2) Niaz, S.; Manzoor, T.; Pandith, A. H. Hydrogen storage: Materials, methods and perspectives. *Renew. Sust. Energy Rev.* **2015**, *50*, 457−469.

(3) Kannah, R. Y.; Kavitha, S.; Preethi; Karthikeyan, O. P.; Kumar, G.; Dai-Viet, N. V.; Banu, J. R. Techno economic assessment of various hydrogen production methods − A review. *Bioresour. Technol.* **2021**, *319*, No. 124175.

(4) Amin, M.; Butt, A. S.; Ahmad, J.; Lee, C.; Azam, S. U.; Mannan, H. A.; Naveed, A. B.; Farooqi, Z. U. R.; Chung, E.; Iqbal, A. Issues and challenges in hydrogen separation technologies. *Energy Rep.* **2023**, *9*, 894−911.

(5) https://energy.ec.europa.eu/topics/energy-systems-integration/hydrogen_en.

(6) Boretti, A.; Banik, B. K. Advances in Hydrogen Production from Natural Gas Reforming. *Adv. Energy Sustainability Res.* **2021**, *2*, 2100097.

(7) Kim, S. H.; Kumar, G.; Chen, W. H.; Khanal, S. K. Renewable hydrogen production from biomass and wastes (ReBioH2−2020). *Bioresour. Technol.* **2021**, *331*, No. 125024.

(8) Koroneos, C.; Katopodi, E. Maximization of wind energy penetration with the use of H_2 production—An exergy approach. *Renew. Sust. Energy Rev.* **2011**, *15*, 648−656.

(9) Sherman, B. D.; McMillan, N. K.; Willinger, D.; Leem, G. Sustainable hydrogen production from water using tandem dye-sensitized photoelectrochemical cells. *Nano Converg.* **2021**, *8*, 7.

(10) Abdalla, A. M.; Hossain, S.; Nisfindy, O. B.; Azad, A. T.; Dawood, M.; Azad, A. K. Hydrogen production, storage, transportation and key challenges with applications: A review. *Energy Convers. Manag.* **2018**, *165*, 602−627.

(11) Rambhujun, N.; Salman, M. S.; Wang, T.; Pratthana, C.; Sapkota, P.; Costalin, M.; Lai, Q.; Aguey-Zinsou, K. F. Renewable hydrogen for the chemical industry. *MRS Energy Sustain.* **2020**, *7*, E33.

(12) National Research Council and National Academy of Engineering *The Hydrogen Economy: Opportunities, Costs, Barriers, and R&D Needs*, The National Academies Press, Washington, DC, 2004.

(13) Tanksale, A.; Beltramini, J. N.; Lu, G. Q. M. A review of catalytic hydrogen production processes from biomass. *Renew. Sust. Energy Rev.* **2010**, *14*, 166−182.

(14) Okolie, J. A.; Patra, B. R.; Mukherjee, A.; Nanda, S.; Dalai, A. K.; Kozinski, J. A. Futuristic applications of hydrogen in energy, biorefining, aerospace, pharmaceuticals and metallurgic. *Int. J. Hydrog. Energy* **2021**, *46*, 8885−8905.

(15) Ustolin, F.; Campari, A.; Taccani, R. An Extensive Review of Liquid Hydrogen in Transportation with Focus on the Maritime Sector. *J. Mar. Sci. Eng.* **2022**, *10*, 1222.
(16) Sun, J.; Feng, H.; Xu, J.; Jin, H.; Guo, L. Investigation of the conversion mechanism for hydrogen production by coal gasification in supercritical water. *Int. J. Hydrog. Energy* **2021**, *46*, 10205−10215.
(17) Matzen, M. J.; Alhajji, M. H.; Demirel, Y. Technoeconomics and Sustainability of Renewable Methanol and Ammonia Productions Using Wind Power-based Hydrogen. *J. Adv. Chem. Eng.* **2015**, *5*, 1000128.
(18) Midilli, A.; Kucuk, H.; Topal, M. E.; Akbulut, U.; Dincer, I. A comprehensive review on hydrogen production from coal gasification: Challenges and Opportunities. *Int. J. Hydrog. Energy* **2021**, *46*, 25385−25412.
(19) Lee, B.; Lim, H. Cost-competitive methane steam reforming in a membrane reactor for H_2 production: Technical and economic evaluation with a window of a H_2 selectivity. *Int. J. Energy Res.* **2019**, *1*, 1−11.
(20) Baharudin, L.; James Watson, M. Hydrogen applications and research activities in its production routes through catalytic hydrocarbon conversion. *Rev. Chem. Eng.* **2017**, *34*, 43−72.
(21) *Steam Reforming* Academic Accelerator https://academic-accelerator.com/encyclopedia/steam-reforming.
(22) *The world is burning more coal than ever before, new report shows* CNN World https://edition.cnn.com/2022/12/16/world/coal-use-record-high-climate-intl/index.html 2022.
(23) Midilli, A.; Kucuk, H.; Haciosmanoglu, M.; Akbulut, U.; Dincer, I. A review on converting plastic wastes into clean hydrogen via gasification for better sustainability. *Int. J. Energy Res.* **2022**, *46*, 4001−4032.
(24) Chen, G.; Jamro, I. A.; Samo, S. R.; Wenga, T.; Baloch, H. A.; Yan, B.; Ma, W. Hydrogen-rich syngas production from municipal solid waste gasification through the application of central composite design: An optimization study. *Int. J. Hydrog. Energy* **2020**, *45*, 33260−33273.
(25) Mansur, F. Z.; Faizal, C. K. M.; Monir, M. U.; Samad, N. A. F. A.; Atnaw, S. M.; Sulaiman, S. A. Co-gasification between coal/sawdust and coal/wood pellet: a parametric study using response surface methodology. *Int. J. Hydrog. Energy* **2020**, *45*, 15963−76.
(26) Basu, P. *Biomass gasification and pyrolysis: practical design and theory*, 1 ed., Academic Press, Oxford, 2010. DOI: 10.1016/B978-0-12-374988-8.00006-4.
(27) Faizan, M.; Song, H. Critical review on catalytic biomass gasification: State-of-Art progress, technical challenges, and perspectives in future development. *Journal of Cleaner Production* **2023**, *408*, No. 137224.
(28) Smart, S.; Lin, C. X. C.; Ding, L.; Thambimuthu, K.; Diniz da Costa, J. C. Ceramic membranes for gas processing in coal gasification. *Energy Environ. Sci.* **2010**, *3*, 268−278.
(29) Novotny, V. From biogas-to hydrogen - Based integrated urban water, energy and waste solids system − Quest towards decarbonization. *Int. J. Hydrogen Energy* **2022**, *47*, 10508−10530.
(30) *Oil & Gases Reports* Offshore Technology https://www.offshore-technology.com/reports.
(31) Khanipour, M.; Mirvakili, A.; Bakhtyari, A.; Farniaei, M.; Rahimpour, M. R. Enhancement of synthesis gas and methanol production by flare gas recovery utilizing a membrane based separation process. *Fuel Process. Technol.* **2017**, *166*, 186−201.
(32) Karousos, D. S.; Qadir, D.; Sapalidis, A. A.; Ahmad, F.; Favvas, E. P. Polymeric, metallic and carbon membranes for hydrogen separation: A review. *Gas Sci. Eng.* **2023**, *120*, No. 205167.
(33) Yáñez, M.; Ortiz, A.; Gorri, D.; Ortiz, I. Comparative performance of commercial polymeric membranes in the recovery of industrial hydrogen waste gas streams. *Int. Jou. Hydr. En.* **2021**, *46*, 17507−17521.
(34) Lei, L.; Bai, L.; Lindbråthen, A.; Pan, F.; Zhang, X.; He, X. Carbon membranes for CO_2 removal: Status and perspectives from materials to processes. *Chem. Eng. J.* **2020**, *401*, No. 126084.
(35) Zito, P. F.; Brunetti, A.; Barbieri, G. Hydrogen concentration and purification by membrane process: a multistage analysis. *Ren. Ene.* **2023**, *218*, No. 119243.
(36) Brunetti, A.; Lei, L.; Avruscio, E.; Karousos, D. S.; Lindbråthen, A.; Kouvelos, E. P.; He, X.; Favvas, E. P.; Barbieri, G. Long-term performance of highly selective carbon hollow fiber membranes for biogas upgrading in presence of H_2S and water vapour. *Chem. Eng. J.* **2022**, *448*, No. 137615.
(37) Lei, L.; Lindbråthen, A.; Hillestad, M.; He, X. Carbon molecular sieve membranes for hydrogen purification from a steam methane reforming process. *J. Membr. Sci.* **2021**, *627*, No. 119241.
(38) Lei, L.; Pan, F.; Lindbråthen, A.; Zhang, X.; Hillestad, M.; Nie, Y.; Bai, L.; He, X.; Guiver, M. D. Carbon hollow fiber membranes for a molecular sieve with precise-cutoff ultramicropores for superior hydrogen separation. *Nat. Commun.* **2021**, *12*, 268.
(39) He, X.; Lei, L.; Dai, Z. Green hydrogen enrichment with carbon membrane processes: Techno-economic feasibility and sensitivity analysis. *Sep. and Purif. Technol.* **2021**, *276*, No. 119346.
(40) Rauch, R.; Hrbek, J.; Hofbauer, H. Biomass gasification for synthesis gas production and applications of the syngas. *Wiley Interdiscip. Rev.: Energy Environ.* **2014**, *3*, 343−362.
(41) Ngamou, P. H. T.; Ivanova, M. E.; Guillon, O.; Meulenberg, W. A. High-performance carbon molecular sieve membranes for hydrogen purification and pervaporation dehydration of organic solvents. *J. Mater. Chem. A* **2019**, *7*, 7082.
(42) Lei, L.; Lindbråthen, A.; Hillestad, M.; Sandru, M.; Favvas, E. P.; He, X. Screening Cellulose Spinning Parameters for Fabrication of Novel Carbon Hollow Fiber Membranes for Gas Separation. *Ind. Eng. Chem. Res.* **2019**, *58*, 13330−13339.
(43) Lei, L.; Lindbråthen, A.; Zhang, X.; Favvas, E. P.; Sandru, M.; Hillestad, M.; He, X. Preparation of carbon molecular sieve membranes with remarkable CO_2/CH_4 selectivity for high-pressure natural gas sweetening. *J. Membr. Sci.* **2020**, *614*, No. 118529.
(44) Zito, P. F.; Brunetti, A.; Drioli, E.; Barbieri, G. CO_2 separation via DDR membrane: mutual influence of mixed gas permeation. *Ind. Eng. Chem. Res.* **2020**, *59*, 7054−7060.
(45) Zito, P. F.; Brunetti, A.; Caravella, A.; Drioli, E.; Barbieri, G. Mutual influence in permeation of CO_2-containing mixtures through a SAPO-34 membrane. *J. Membr. Sci.* **2020**, *595*, No. 117534.
(46) Krishna, R.; van Baten, J. M. Onsager coefficients for binary mixture diffusion in nanopores. *Chem. Eng. Sci.* **2008**, *63*, 3120.
(47) van den Bergh, J.; Ban, S.; Vlugt, T. J. H.; Kapteijn, F. Modeling the loading dependency of diffusion in zeolites: the relevant site model. *J. Phys. Chem. C* **2009**, *113*, 17840.
(48) Doherty, W.; Reynolds, A.; Kennedy, D. The effect of air preheating in a biomass CFB gasifier using ASPEN Plus simulation. *Biomass Bioenergy* **2009**, *33*, 1158−1167.

https://doi.org/10.1021/acssuschemeng.3c08236
ACS Sustainable Chem. Eng. 2024, 12, 3344−3354